

# Oligonucleotide Melting Temperatures under PCR Conditions: Nearest-Neighbor Corrections for $Mg^{2+}$ , Deoxynucleotide Triphosphate, and Dimethyl Sulfoxide Concentrations with Comparison to Alternative Empirical Formulas

NICOLAS VON AHSEN,<sup>1\*</sup> CARL T. WITTEW,<sup>2</sup> and EKKEHARD SCHÜTZ<sup>1,3</sup>

**Background:** Many techniques in molecular biology depend on the oligonucleotide melting temperature ( $T_m$ ), and several formulas have been developed to estimate  $T_m$ . Nearest-neighbor (N-N) models provide the highest accuracy for  $T_m$  prediction, but it is not clear how to adjust these models for the effects of reagents commonly used in PCR, such as  $Mg^{2+}$ , deoxynucleotide triphosphates (dNTPs), and dimethyl sulfoxide (DMSO).

**Methods:** The experimental  $T_m$ s of 475 matched or mismatched target/probe duplexes were obtained in our laboratories or were compiled from the literature based on studies using the same real-time PCR platform. This data set was used to evaluate the contributions of  $[Mg^{2+}]$ ,  $[dNTPs]$ , and  $[DMSO]$  in N-N calculations. In addition, best-fit coefficients for common empirical formulas based on GC content, length, and the equivalent sodium ion concentration of cations  $[Na^+_{eq}]$  were obtained by multiple regression.

**Results:** When we used  $[Na^+_{eq}] = [Monovalent\ cations] + 120(\sqrt{[Mg^{2+}]} - [dNTPs])$  (the concentrations in this formula are mmol/L) to correct  $\Delta S^0$  and a DMSO term of 0.75 °C (%DMSO), the SE of the N-N  $T_m$  estimate was 1.76 °C for perfectly matched duplexes ( $n = 217$ ). Alternatively, the empirical formula  $T_m$  (°C) =  $77.1\text{ °C} + 11.7 \times \log[Na^+_{eq}] + 0.41(\%GC) - 528/bp - 0.75\text{ °C}(\%DMSO)$  gave a slightly higher SE of 1.87 °C.

When all duplexes (matched and mismatched;  $n = 475$ ) were included in N-N calculations, the SE was 2.06 °C.

**Conclusions:** This robust model, accounting for the effects of  $Mg^{2+}$ , DMSO, and dNTPs on oligonucleotide  $T_m$  in PCR, gives reliable  $T_m$  predictions using thermodynamic N-N calculations or empirical formulas.

© 2001 American Association for Clinical Chemistry

DNA amplification and detection techniques often depend on oligonucleotide melting temperature ( $T_m$ ).<sup>4</sup> The  $T_m$  of a DNA duplex, defined as the temperature where one-half of the nucleotides are paired and one-half are unpaired (1), corresponds to the midpoint of the spectroscopic hyperchromic absorbance shift during DNA melting (2). The  $T_m$  indicates the transition from double helical to random coil formation and is related to the DNA GC base content (2). Other important factors for DNA stability are the cation concentration of the surrounding buffer (3, 4) and the DNA double strand length (5). The  $T_m$  of polymer DNA can be predicted by formulas that account for differing GC content in various buffers (6). A term for the length of the duplex can also be included (1, 7, 8).

The most accurate prediction of  $T_m$  for oligonucleotide DNA uses the thermodynamic nearest-neighbor (N-N) model [see Ref. (9) for review and parameters]. N-N calculations for  $T_m$  prediction are useful on microarrays (10) and for the selection of PCR primers and hybridization probes (11). Empirical data from probe melting curve analysis during real-time PCR correlate well with theoretical predictions (12, 13). The N-N model is based on the

<sup>1</sup> Department of Clinical Chemistry, Georg-August University, Robert Koch Strasse 40, 37075 Goettingen, Germany.

<sup>2</sup> Department of Pathology, University of Utah Medical School, Salt Lake City, UT 84132.

<sup>3</sup> Chronic Illness Research Foundation, San Francisco, CA 94107.

\*Author for correspondence. Fax 49-551-39-12504; e-mail nahsen@gwdg.de.

Received July 6, 2001; accepted August 17, 2001.

<sup>4</sup> Nonstandard abbreviations:  $T_m$ , melting temperature; N-N, nearest-neighbor; dNTP, deoxynucleotide triphosphate; and DMSO, dimethyl sulfoxide.

assumption that probe hybridization energy can be calculated from the enthalpy and entropy of all N-N pairs, including a contribution from each dangling end. Thermodynamic values for entropy and enthalpy of each possible matched N-N and dangling ends have been determined (9, 14). Dangling-end effects account for the stacking energy of a shorter probe on a more lengthy target (15, 16). The entropy ( $\Delta S$ ) is salt dependent, and  $\Delta S^0$  must be corrected if the ionic environment is different from 1 mol/L NaCl, the salt concentration at which most thermodynamic values have been derived. However,  $Mg^{2+}$  is present in PCR as an important cofactor for Taq DNA polymerase and strongly influences  $\Delta S$  (17). Deoxynucleotide triphosphates (dNTPs) are also essential and chelate some of the available  $Mg^{2+}$  (18). In addition, dimethyl sulfoxide (DMSO) is commonly used as a cosolvent (19) to facilitate amplification from difficult templates. Addition of DMSO decreases the  $T_m$  (20–22), which must be taken into account when primer  $T_m$  is calculated (23).

To get a deeper insight into probe  $T_m$  under common PCR buffer conditions, we have compiled  $T_m$  data from 475 different DNA duplexes. These assays were performed with different concentrations of  $Mg^{2+}$  and DMSO, reflecting current PCR laboratory practice. We provide an empirical  $\Delta S$  compensation for the  $Mg^{2+}$  and dNTP influence on ionic strength. In addition, best-fit coefficients for simpler formulas based on GC content, length, and the equivalent sodium ion concentration are determined for convenient bench-side use that offer accurate  $T_m$  predictions.

## Materials and Methods

### BASIC PRINCIPLE

The LightCycler real-time PCR machine (Roche Molecular Biochemicals) is capable of detecting the hybridization of adjacent fluorescent dye-labeled probes by fluorescence resonance energy transfer (24). Assay design for the detection of single nucleotide polymorphisms requires that the sensor probe (the probe covering the mutation) has a lower  $T_m$  than the detection probe, which stays hybridized during the melting cycle. The observed  $T_m$ s from matched and mismatched hybridizations can be predicted using the N-N model (12). Probes have a  $T_m$  similar to PCR primers (50–70 °C), and the results from probe  $T_m$  prediction can also be used to predict primer  $T_m$ s, a critical parameter for PCR performance (23, 25–27).

### DATA COLLECTION

All assays were performed using the LightCycler real-time PCR instrument. Most  $T_m$ s were measured in our laboratories ( $n = 388$ ) during the course of genotyping experiments [for examples, see Refs (12, 28)]. Some additional  $T_m$ s were extracted from the literature when complete experimental conditions were published ( $n = 87$ ). In total, 162 different probes were used with various templates and conditions, including 221 completely matched

hybridizations, 237 single mismatches, and 17 two-point mismatches. Forty assays were based on melting curves detected with SYBR Green I, whereas the remainder were based on the melting of fluorescent oligonucleotide probes. DMSO was used in 206 assays in concentrations ranging from 2.5% to 10%. These data are available as an online supplement at *Clinical Chemistry Online* (<http://www.clinchem.org/content/vol47/issue11>).

### STATISTICAL ANALYSIS

*N-N calculations.* The entropy and enthalpy were calculated from probe sequences at standard conditions (1 mol/L NaCl) as described in more detail elsewhere (9, 29, 30). In addition we considered the published thermodynamic data for dangling-end contributions (14). Mismatches were accounted for by the thermodynamic data reported by Allawi and SantaLucia (31–34) and Peyret et al. (35). The PCR DNA target concentration was set to 50 nM. SYBR Green I, if present, was assumed to increase the  $T_m$  by 1 °C at 1:20 000 dilution, based on own preliminary data. Calculations were performed with Excel™ for Windows (Microsoft), using the built-in statistical functions. The Pearson  $r^2$  was used for correlations, and standard linear regression was used for relating observed to measured  $T_m$ . Thermodynamic N-N stability calculations were performed using MeltCalc, a spreadsheet software for Excel (36).

The observed  $T_m$  was used as the dependent variable in a multiple variable fit to determine the DMSO coefficient and the best formula for  $Mg^{2+}$  influence. Prior evidence suggested that the influence of  $Mg^{2+}$  on  $T_m$  is stoichiometrically reduced by dNTPs. Initial calculations based on  $r^2$  indicated that the relationship of DMSO to  $T_m$  was linear, whereas  $[Mg^{2+}]$  was nonlinear. Therefore, our model was:  $T_m$  (observed) =  $T_m$  (predicted) –  $a \times \text{DMSO}$  (%), with  $[\text{Na}^+_{\text{eq}}] = [\text{monovalent cations}] + b \times ([Mg^{2+}] - [\text{dNTP}])^c$ . The parameters  $a$ ,  $b$ , and  $c$  were optimized to minimize the prediction error by stepwise incremental iterations. With  $a = 0.75$ ,  $b = 120$ , and  $c = 0.5$ , only 18% of the predicted values fell outside a 5% error limit. The nonlinear effect of  $[Mg^{2+}]$  on  $[\text{Na}^+_{\text{eq}}]$  was best approximated by the square-root function, which is in agreement with a previous report (37).

*Alternative formulas.* Using our empirical data set, we evaluated several simpler formulas for their ability to predict  $T_m$ . These formulas cannot properly account for the presence of single mismatches. Therefore, only data for matched probe/template duplexes were used.

The Wallace–Ikatura rule is often used as a rule of thumb when primer  $T_m$  is to be estimated at the bench (1, 38). However, the formula was originally applied to the hybridization of probes in 1 mol/L NaCl (1) and is an estimate of the denaturation temperature ( $T_d$ ):

$$T_d (\text{°C}) = 2(A + T) + 4(G + C) \quad (1)$$

Another equation for the effective priming temperature ( $T_p$ ) was suggested by Wu et al. (25):

$$T_p (\text{°C}) = 22 + 1.46L_n \quad (2)$$

where  $L_n = 2(G + C) + (A + T)$ .

Marmur and Doty (2) originally established a formula to correlate GC content (%GC) to the  $T_m$  of long duplexes at a given ionic strength. Chester and Marshak (23) added a term to account for DNA strand length ( $n$  in base pairs) to estimate primer  $T_m$ :

$$T_m = 69.3 + 0.41(\%GC) - 650/n \quad (3)$$

The Marmur–Schildkraut–Doty equation also accounts for ionic strength with a term for the Na<sup>+</sup> concentration (1, 2, 6–8).

$$T_m (\text{°C}) = 81.5 \text{ °C} + 16.6(\log[\text{Na}^+]) + 0.41(\%GC) - b/n \quad (4)$$

Values between 500 and 750 have been used for  $b$  (5, 23), a value that may increase with the ionic strength (8).

Another modification is that of Wetmur (1):

$$T_m = 81.5 + 16.6 \times \log\left(\frac{[\text{Na}^+]}{1.0 + 0.7 \times [\text{Na}^+]}\right) + 0.41(\%GC) - 500/n \quad (5)$$

Eqs. 4 and 5 assume that the stabilizing effects of cations are the same on all base pairs. However, Owen et al. (39) observed that the slopes of  $T_m$  vs  $\log[\text{Na}^+]$  decrease with increasing GC content, leading to the following final formula for the estimation of  $T_m$  in polymer DNA (40–42):

$$T_m (\text{°C}) = 87.16 + 0.345(\%GC) + \log[\text{Na}^+] \times [20.17 - 0.066(\%GC)] \quad (6)$$

## Results

### DESCRIPTIVE STATISTICS

Empirical oligonucleotide  $T_m$ s were obtained under 475 unique conditions typical of current PCR practice. The Mg<sup>2+</sup> concentration was 1–6 mM (mean,  $2.9 \pm 1.17$  mM), the length of the probes was 11–45 bp (median, 19 bp), and the GC content was 17–88% (mean,  $52.5\% \pm 9.6\%$ ). DMSO was used in 206 assays in concentrations ranging from 2.5% to 10%. In 57 assays, synthesized oligonucleotides were used without PCR. Probe concentrations were 0.025–0.5  $\mu\text{M}$  (mean,  $0.15 \pm 0.087$   $\mu\text{M}$ ). The monovalent cation concentration was 20–54 mM, depending on the PCR buffer system. The measured probe  $T_m$ s varied from 43.2 to 74.7 °C (mean,  $59.1 \pm 6.42$  °C).

### STATISTICAL ANALYSIS

*N-N calculations.* The best fit values for [Mg<sup>2+</sup>] and [dNTP] coefficients revealed that the Na<sup>+</sup> equivalents (Na<sup>+</sup><sub>eq</sub>) were approximated by:

$$[\text{Na}^+_{\text{eq}}] = [\text{Monovalent cations}] + 120(\sqrt{[\text{Mg}^{2+}] - [\text{dNTPs}]}) \quad (7)$$

Note that the concentrations in Eq. 7 are in mmol/L. In all other equations, concentrations are in mol/L. Monovalent cations are typically present as K<sup>+</sup> and Tris<sup>+</sup> in PCR buffer (18, 26). K<sup>+</sup> is similar to Na<sup>+</sup> in regard to duplex stabilization (17).  $\Delta S^0$  was corrected for the salt concentration as follows (9):

$$S^0[\text{Na}^+] = S^0[1 \text{ M Na}^+] + 0.847 \times n \times \log[\text{Na}^+] \quad (8)$$

where  $n$  is the total number of phosphates in the duplex divided by 2. This is equal to the oligonucleotide length minus 1.

Each percentage of DMSO (by volume) decreased the  $T_m$  by 0.75 °C. GC content had no obvious influence on the DMSO factor. Using these equations, we found a good regression of predicted vs observed  $T_m$  (Fig. 1). The mean prediction error was  $0.2 \pm 2.18$  °C, which is within the error range for N-N calculations.

*Alternative formulas.* The Wallace–Ikatura rule (Eq. 1) overestimates the  $T_m$  of long duplexes and gives reasonable results only in the range of 14–20 bp (1, 38). Therefore, only duplexes shorter than 21 bp were included in the analysis (Table 1). When the analysis was extended to include duplexes of up to 24 bp,  $r^2$  decreased to 0.64.

The equation for the effective priming temperature by Wu et al. (25) (Eq. 2) is similar to the Wallace–Ikatura rule. Only oligonucleotides with  $L_n < 39$  (see Eq. 2) were included in the analysis, as suggested by the authors. The oligonucleotide  $T_m$  is overestimated by a mean of 2.5 °C by this formula (Table 1).

Including the length dependence of Chester and Marshak [Eq. 3; (23)] improved  $r^2$ , but the intercept and

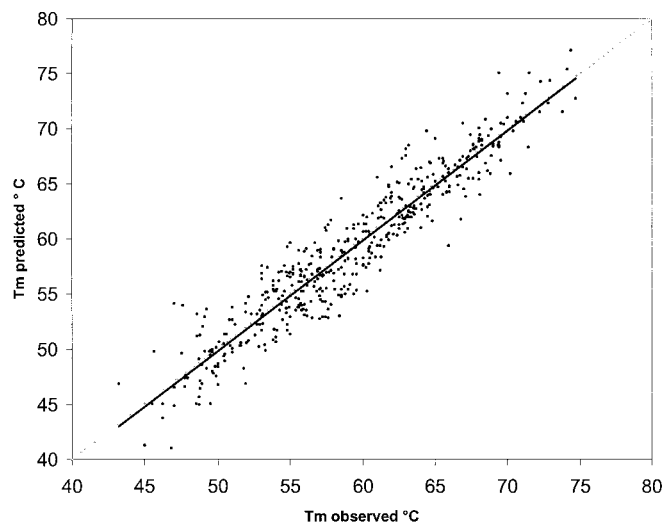


Fig. 1. Observed vs predicted  $T_m$  for 475 melting temperature assays. (---), line of identity; (—), regression line:  $y = 1.00x - 0.29$ .

**Table 1. Comparison of the predictive performance of different equations for the calculation of oligonucleotide  $T_m$ .<sup>a</sup>**

	N-N calculations		Equation					
	Including mismatches	Without mismatches	1 <sup>b</sup>	2 <sup>c</sup>	9	10	11	12
n	475	217	131	200	217	217	217	217
$r^2$	0.90	0.89	0.78	0.60	0.86	0.87	0.88	0.88
Slope	1.00	1.05	1.20	0.95	1.01	0.96	0.97	1.01
Intercept, $\Delta T_m$	-0.29	-3.17	-18.44	5.83	-0.60	2.65	2.32	-0.54
$S_{y,x}$	2.06	1.76	2.21	3.13	1.99	1.88	1.87	1.86
Mean $\pm$ SD of differences (observed minus predicted)	0.1 $\pm$ 2.18	0.2 $\pm$ 1.96	6.1 $\pm$ 3.13	-2.5 $\pm$ 3.84	-0.1 $\pm$ 1.93	0.0 $\pm$ 2.16	-0.1 $\pm$ 2.00	0.1 $\pm$ 2.18

<sup>a</sup> See *Materials and Methods* for a detailed description of the formulas.  
<sup>b</sup> Only oligonucleotides <21 bp were included in the analysis.  
<sup>c</sup> Only oligonucleotides with  $L_n < 39$  (see Eq. 2) were included in the analysis.

difference between observed and predicted  $T_m$ s were poor (data not shown). However, a better fit was obtained with new constants obtained from stepwise iterations (fit variable: length dependency term):

$$T_m = 69.3 + 0.41(\%GC) - 535/n \quad (9)$$

To improve Eq. 4, a  $dT_m/d\log[Na^+]$  of 11.7 °C was used as suggested for oligonucleotide DNA (9) instead of the commonly used 16.6 °C (6). Best-fit values for the temperature offset and length dependence were then obtained by stepwise iterations (fit variables:  $T_m$  offset, length dependency term):

$$T_m (\text{°C}) = 77.1 \text{ °C} + 11.7 \times \log[Na^+] + 0.41(\%GC) - 528/n \quad (10)$$

In the same manner, the modification for the formula of Wetmur (1) is (fit variables:  $T_m$  offset, length dependency term):

$$T_m = 77.8 + 11.7 \times \log\left(\frac{[Na^+]}{1.0 + 0.7 \times [Na^+]}\right) + 0.41(\%GC) - 528/n \quad (11)$$

The fit of this equation could not be improved (data not shown) by the introduction of a salt dependence term for  $b$  (see Eq. 4) as suggested previously (8).

Eq. 6 has been suggested as the best predictor of polymer DNA  $T_m$  (41, 42). The best fit of constants in this formula based on our oligonucleotide data produced (fit variables:  $T_m$  offset, oligomer  $[Na^+]$  dependency term, length dependency term added):

$$T_m (\text{°C}) = 80.4 + 0.345(\%GC) + \log[Na^+] \times [17.0 - 0.135(\%GC)] - 550/n \quad (12)$$

### Discussion

Many techniques in modern molecular biology depend on oligonucleotide duplex formation. Perhaps the most universal method in use today is the PCR, with applications

including amplification, cloning, mutation detection, and mutagenesis. A precise knowledge of oligonucleotide  $T_m$  is useful for rapid optimization of assays. The most accurate predictions of oligonucleotide  $T_m$ s use the N-N model. N-N parameters have recently been improved (9), and their ability to predict the  $T_m$  of unknown oligonucleotide duplexes demonstrated (30). However, these parameters usually are determined in 1 mol/L NaCl and need to be corrected for the conditions in the PCR. Although correction factors for different NaCl concentrations have been published (9), we are not aware of an investigation into nucleic acid stability under typical PCR buffer conditions, even given its high practical value. It is well appreciated that  $Mg^{2+}$  stabilizes duplex DNA 80- to 100-fold (3) to as much as 140-fold (17) more than  $Na^+$ . Our findings indicate a nonlinear effect of  $[Mg^{2+}]$  on  $[Na^+_{eq}]$  in the order of  $120(\sqrt{[Mg^{2+}]})$ .

The N-N model accurately predicts probe  $T_m$  in the LightCycler analysis system (12). We compiled and analyzed measured  $T_m$  data for matched and mismatched hybridization probes from different laboratories. Therefore, some interlaboratory variation is expected from different reagents and protocols. The temperature transition rates during melting curve acquisition (usually 0.1–0.2 °C/s) are too fast to achieve equilibrium conditions and cause a slight overestimation of the true  $T_m$  (43).

Probe sequence choices reflect the demands of mutation detection and are not designed particularly for two-state behavior. Even with these limitations, the predictive accuracy we have achieved underscores the robustness of the parameterization. Systematic errors introduced by fluorescent dyes were negligible in another study (10), and fluorescence resonance energy transfer probes themselves have successfully been used to derive thermodynamic parameters (44). Our findings should be equally applicable to probe and primer oligonucleotides, thereby allowing in silico optimization of primers and probes, saving both on time required for optimization and costs for probe resynthesis (12, 29, 45–47).

An extensive survey of alternative formulas used for

the prediction of perfectly matched oligonucleotide DNA was also performed. The Wallace–Ikatura rule (Eq. 1) is often used as a rough predictor of primer  $T_m$  but has limited accuracy, especially for longer oligonucleotides. This rule assumes a salt concentration of 1 mol/L NaCl, which is typical for dot blots and other hybridizations but not PCR. The fact that it is used for PCR applications is more a testament of the robustness of PCR toward different annealing temperatures than evidence for accurate  $T_m$  estimates. The same is true for the formula of Wu et al. (25). Many formulas were originally designed to relate measured  $T_m$  and GC content of polymer DNA (Eqs. 3–6). The inclusion of additional terms for ionic strength (6), length dependency (5), and GC dependency of ionic strength (39) has led to more accurate estimates for polymer DNA. Eqs. 9–12 have been specifically optimized for oligonucleotide  $T_m$  estimation by best-fit estimates of our data set. Eq. 10 is recommended as a tradeoff between accuracy and ease of use. Table 2 gives primer  $T_m$ s for common primer compositions and PCR conditions. These estimates may not be accurate for certain sequences with a biased N-N composition (41). Furthermore, mismatches are strongly dependent on their N-N bases and require more laborious N-N calculations.

The effect of DMSO on thermal stability of DNA has been investigated before. Our factor of 0.75 °C decrease in  $T_m$  per 1% DMSO is similar to previous findings of 0.6 °C per 1% DMSO (20), 0.675 °C per 1% DMSO (22), and 0.5 °C per 1% DMSO (21). These prior studies were performed on polymer DNA, suggesting that DMSO may have a slightly greater effect on oligomer DNA.

Because template priming during PCR is a kinetic process, efficient, specific priming should occur at the

primer  $T_m$  (25), suggesting that the  $T_m$  can be used as the annealing temperature in PCR. Because efficient amplification is dependent on hybridization of both primers, it is rational to use the  $T_m$  of the least stable primer. The temperature used for annealing in PCR also depends on the annealing time. For example, allele-specific amplification can be achieved with rapid cycling (“0” s annealing) at a lower annealing temperature than conventional cycling with a longer annealing time (48). Finally,  $T_m$  is not just a property of an oligonucleotide, but a property of an oligonucleotide under specific conditions and at a given concentration.

In conclusion, we have developed a robust model for the effects of Mg<sup>2+</sup>, DMSO, and dNTPs on oligonucleotide  $T_m$  under common PCR buffer conditions. This enables reliable  $T_m$  predictions and in silico primer and probe optimization using thermodynamic N-N calculations. We performed an extensive evaluation of different equations advocated for PCR primer  $T_m$  prediction. These formulas have been parameterized to accommodate for standard PCR conditions and are now useful for rapid calculation of the  $T_m$  of perfectly matched oligonucleotides. It is rational to use the  $T_m$  of the least stable PCR primer as the annealing temperature in PCR.

The MeltCalc software is copyrighted by Ekkehard Schütz and Nicolas von Ahsen.

## References

**Table 2. Standard primer  $T_m$ s (°C) calculated for different lengths, Mg<sup>2+</sup> concentration, and GC content at 0.8 mM dNTPs and 50 mM monovalent ion concentration without mismatches and with no addition of cosolvents.<sup>a</sup>**

%GC	Mg <sup>2+</sup> , mM	$T_m$ , °C			
		18 bp	20 bp	22 bp	24 bp
40	1.0	52.6	55.6	58.0	60.0
	1.5	54.5	57.5	59.9	61.9
	2.0	55.5	58.4	60.8	62.8
	2.5	56.2	59.1	61.5	63.5
	3.0	56.7	59.6	62.0	64.0
50	1.0	56.7	59.7	62.1	64.1
	1.5	58.6	61.6	64.0	66.0
	2.0	59.6	62.5	64.9	66.9
	2.5	60.3	63.2	65.6	67.6
	3.0	60.8	63.7	66.1	68.1
60	1.0	60.8	63.8	66.2	68.2
	1.5	62.7	65.7	68.1	70.1
	2.0	63.7	66.6	69.0	71.0
	2.5	64.4	67.3	69.7	71.7
	3.0	64.9	67.8	70.2	72.2

<sup>a</sup> Eqs. 7 and 10 (see *Material and Methods*) were used for the calculations.

1. Wetmur JG. DNA probes: applications of the principles of nucleic acid hybridization. *Crit Rev Biochem Mol Biol* 1991;26:227–59.
2. Marmur J, Doty P. Determination of the base composition of deoxyribonucleic acid from its thermal denaturation temperature. *J Mol Biol* 1962;5:109–18.
3. Thomas R. [Investigations into denaturation of DNA]. *Biochim Biophys Acta* 1954;14:231–40.
4. Dove WF, Davidson N. Cation effects on the denaturation of DNA. *J Mol Biol* 1962;5:467–78.
5. Hall TJ, Grula JW, Davidson EH, Britten RJ. Evolution of sea urchin non-repetitive DNA. *J Mol Evol* 1980;16:95–110.
6. Schildkraut C, Lifson S. Dependence of the melting temperature of DNA on salt concentration. *Biopolymers* 1965;3:195–208.
7. Wahl GM, Berger SL, Kimmel AR. Molecular hybridization of immobilized nucleic acids: theoretical concepts and practical considerations. *Methods Enzymol* 1987;152:399–407.
8. Britten RJ, Graham DE, Neufeld BR. Analysis of repeating DNA sequences by reassociation. *Methods Enzymol* 1974;29:363–418.
9. SantaLucia J Jr. A unified view of polymer, dumbbell, and oligonucleotide DNA nearest-neighbor thermodynamics. *Proc Natl Acad Sci U S A* 1998;95:1460–5.
10. Fotin AV, Drobyshev AL, Proudnikov DY, Perov AN, Mirzabekov AD. Parallel thermodynamic analysis of duplexes on oligodeoxyribonucleotide microchips. *Nucleic Acids Res* 1998;26:1515–21.
11. Rychlik W, Rhoads RE. A computer program for choosing optimal oligonucleotides for filter hybridization, sequencing and in vitro amplification of DNA. *Nucleic Acids Res* 1989;17:8543–51.
12. von Ahsen N, Oellerich M, Armstrong VW, Schütz E. Application of

- a thermodynamic nearest-neighbor model to estimate nucleic acid stability and optimize probe design: prediction of melting points of different mutations of apolipoprotein B 3500 and factor V Leiden with a hybridization probe genotyping assay on the LightCycler. *Clin Chem* 1999;45:2094–101.
13. von Ahsen N, Oellerich M, Schütz E. DNA base bulge vs unmatched end formation in probe-based diagnostic insertion/deletion genotyping: genotyping the *UGT1A1* (TA)<sub>n</sub> polymorphism by real-time fluorescence PCR. *Clin Chem* 2000;46:1939–45.
  14. Bommarito S, Peyret N, SantaLucia J Jr. Thermodynamic parameters for DNA sequences with dangling ends. *Nucleic Acids Res* 2000;28:1929–34.
  15. Hayes FN, Lilly EH, Ratliff RL, Smith DA, Williams DL. Thermal transitions in mixtures of polydeoxyribonucleotides. *Biopolymers* 1970;9:1105–17.
  16. Lane MJ, Paner T, Kashin I, Faldasz BD, Li B, Gallo FJ, et al. The thermodynamic advantage of DNA oligonucleotide 'stacking hybridization' reactions: energetics of a DNA nick. *Nucleic Acids Res* 1997;25:611–7.
  17. Nakano S, Fujimoto M, Hara H, Sugimoto N. Nucleic acid duplex stability: influence of base composition on cation effects. *Nucleic Acids Res* 1999;27:2957–65.
  18. Baumforth KR, Nelson PN, Digby JE, O'Neil JD, Murray PG. Demystified . . . the polymerase chain reaction. *Mol Pathol* 1999; 52:1–10.
  19. Pomp D, Medrano JF. Organic solvents as facilitators of polymerase chain reaction. *Biotechniques* 1991;10:58–9.
  20. Musielski H, Mann W, Laue R, Michel S. Influence of dimethylsulfoxide on transcription by bacteriophage T3- induced RNA polymerase. *Z Allg Mikrobiol* 1981;21:447–56.
  21. Cullen BR, Bick MD. Thermal denaturation of DNA from bromodeoxyuridine substituted cells. *Nucleic Acids Res* 1976;3:49–62.
  22. Escara JF, Hutton JR. Thermal stability and renaturation of DNA in dimethyl sulfoxide solutions: acceleration of the renaturation rate. *Biopolymers* 1980;19:1315–27.
  23. Chester N, Marshak DR. Dimethyl sulfoxide-mediated primer  $T_m$  reduction: a method for analyzing the role of renaturation temperature in the polymerase chain reaction. *Anal Biochem* 1993;209: 284–90.
  24. de Silva D, Wittwer CT. Monitoring hybridization during polymerase chain reaction. *J Chromatogr B* 2000;741:3–13.
  25. Wu DY, Ugozzoli L, Pal BK, Qian J, Wallace RB. The effect of temperature and oligonucleotide primer length on the specificity and efficiency of amplification by the polymerase chain reaction. *DNA Cell Biol* 1991;10:233–8.
  26. Saiki RK, Gelfand DH, Stoffel S, Scharf SJ, Higuchi R, Horn GT, et al. Primer-directed enzymatic amplification of DNA with a thermostable DNA polymerase. *Science* 1988;239:487–91.
  27. Rychlik W, Spencer WJ, Rhoads RE. Optimization of the annealing temperature for DNA amplification in vitro [published erratum appears in *Nucleic Acids Res* 1991;19:698]. *Nucleic Acids Res* 1990;18:6409–12.
  28. Crockett AO, Wittwer CT. Fluorescein-labeled oligonucleotides for real-time PCR: using the inherent quenching of deoxyguanosine nucleotides. *Anal Biochem* 2001;290:89–97.
  29. von Ahsen N, Schütz E. Using the nearest neighbor model for the estimation of matched and mismatched hybridization probe melting points and selection of optimal probes on the LightCycler. In: Meuer S, Wittwer C, Nakagawara K-I, eds. *Rapid cycle real time PCR—methods and applications*. Berlin: Springer Verlag, 2001: 43–56.
  30. Owczarzy R, Vallone PM, Gallo FJ, Paner TM, Lane MJ, Benight AS. Predicting sequence-dependent melting stability of short duplex DNA oligomers. *Biopolymers* 1997;44:217–39.
  31. Allawi HT, SantaLucia J Jr. Thermodynamics and NMR of internal G\*T mismatches in DNA. *Biochemistry* 1997;36:10581–94.
  32. Allawi HT, SantaLucia J Jr. Nearest-neighbor thermodynamics of internal A\*C mismatches in DNA: sequence dependence and pH effects. *Biochemistry* 1998;37:9435–44.
  33. Allawi HT, SantaLucia J Jr. Thermodynamics of internal C\*T mismatches in DNA. *Nucleic Acids Res* 1998;26:2694–701.
  34. Allawi HT, SantaLucia J Jr. Nearest neighbor thermodynamic parameters for internal G\*A mismatches in DNA. *Biochemistry* 1998;37:2170–9.
  35. Peyret N, Seneviratne PA, Allawi HT, SantaLucia J Jr. Nearest-neighbor thermodynamics and NMR of DNA sequences with internal A\*A, C\*C, G\*G, and T\*T mismatches. *Biochemistry* 1999;38:3468–77.
  36. Schütz E, von Ahsen N. Spreadsheet software for thermodynamic melting point prediction of oligonucleotide hybridization with and without mismatches. *Biotechniques* 1999;27:1218–24.
  37. Wetmur JG. Nucleic acid hybrids, formation and structure of. In: Meyers RA, ed. *Encyclopedia of molecular biology and molecular medicine*, Vol. 4. Weinheim, Germany: VCH Verlagsgesellschaft, 1996:235–43.
  38. Meinkoth J, Wahl G. Hybridization of nucleic acids immobilized on solid supports. *Anal Biochem* 1984;138:267–84.
  39. Owen RJ, Hill LR, Lapage SP. Determination of DNA base compositions from melting profiles in dilute buffers. *Biopolymers* 1969; 7:503–16.
  40. Frank-Kamenetskii MD. Simplification of the empirical relationship between melting temperature of DNA, its GC content and concentration of sodium ions in solution. *Biopolymers* 1971;10:2623–4.
  41. Blake RD. Denaturation of DNA. In: Meyers RA, ed. *Encyclopedia of molecular biology and molecular medicine*, Vol. 2. Weinheim, Germany: VCH Verlagsgesellschaft, 1996:1–19.
  42. Blake RD, Delcourt SG. Thermal stability of DNA. *Nucleic Acids Res* 1998;26:3323–32.
  43. Gundry CN, Bernard PS, Herrmann MG, Reed GH, Wittwer CT. Rapid F508del and F508C assay using fluorescent hybridization probes. *Genet Test* 1999;3:365–70.
  44. Gelfand CA, Plum GE, Mielewczyk S, Remeta DP, Breslauer KJ. A quantitative method for evaluating the stabilities of nucleic acids. *Proc Natl Acad Sci U S A* 1999;96:6113–8.
  45. Schütz E, von Ahsen N, Oellerich M. Genotyping of eight thiopurine methyltransferase mutations: three-color multiplexing, "Two-Color/Shared" anchor, and fluorescence-quenching hybridization probe assays based on thermodynamic nearest-neighbor probe design. *Clin Chem* 2000;46:1728–37.
  46. Schütz E, von Ahsen N. Genotyping the most common thiopurine methyltransferase mutations with the LightCycler. In: Meuer S, Wittwer C, Nakagawara K-I, eds. *Rapid cycle real time PCR—methods and applications*. Berlin: Springer Verlag, 2001:143–52.
  47. von Ahsen N, Oellerich M, Schütz E. A method for homogeneous color-compensated genotyping of factor V (G1691A) and methyl-entetrahydrofolate reductase (C677T) mutations using real-time multiplex fluorescence PCR. *Clin Biochem* 2000;33:535–9.
  48. Wittwer CT, Marshall BC, Reed GH, Cherry JL. Rapid cycle allele-specific amplification: studies with the cystic fibrosis  $\Delta F508$  locus. *Clin Chem* 1993;39:804–9.